

# Energy transfer along the reconstructed quantum Hall edge

E.V. Deviatov,<sup>1,\*</sup> A. Lorke,<sup>2</sup> G. Biasiol,<sup>3</sup> and L. Sorba<sup>4</sup>

<sup>1</sup>*Institute of Solid State Physics RAS, Chernogolovka, Moscow District, 142432, Russia*

<sup>2</sup>*Laboratorium für Festkörperphysik, Universität Duisburg-Essen, Lotharstr. 1, D-47048, Duisburg, Germany*

<sup>3</sup>*IOM CNR, Laboratorio TASC, 34149 Trieste, Italy*

<sup>4</sup>*NEST, Istituto Nanoscienze-CNR and Scuola Normale Superiore, 56127 Pisa, Italy*

(Dated: January 26, 2023)

We use a novel sample design, which is based on the highly imbalanced co-propagating edge states, to independently investigate a charge and an energy transport along the smooth sample edge. We experimentally observe an energy transfer contrary to the electrons' drift for the filling factors 1 and 1/3. Our analysis indicates that a neutral collective mode at the smooth interaction-reconstructed edge is a proper candidate for the experimentally observed effect.

PACS numbers: 73.40.Qv 71.30.+h

Recent interest [1, 2] to the energy transport along the edge of the quantum Hall system originates from the problem of counter-propagating neutral modes, with the latter carrying only energy. Neutral modes were not observed in a direct heat-transport experiment [1], however, they were detected in the short-noise measurements [2]. This discrepancy might originate from different experimental methods in Refs. [1, 2], so an independent investigation is necessary in another experimental configuration.

The charged collective modes are propagating in the direction of electrons' drift along the quantum Hall edge. It was proposed [3], that at some fractional filling factors  $\nu = 2/3, 5/2$  interaction leads to counter-propagating neutral modes. For the smooth sample edge, the reconstruction is predicted [4] even for simplest  $\nu = 1, 1/3$  as a result of the interplay between the smooth edge potential and the Coulomb interaction energy. The reconstructed edge is characterized by oscillations of density profile, which allows [4] counter-propagating neutral edge modes even at these simplest fillings. Some experimental arguments for the edge reconstruction of this type can also be found in the capacitance measurements at the edges of  $\nu = 1, 1/3$  plateau, where a so-called negative compressibility was experimentally observed [5].

Here, we use a novel sample design, which is based on the highly imbalanced co-propagating edge states, to independently investigate a charge and an energy transport along the smooth sample edge. We experimentally observe an energy transfer contrary to the electrons' drift for the filling factors 1 and 1/3. Our analysis indicates that a neutral collective mode at the smooth interaction-reconstructed edge is a proper candidate for the experimentally observed effect.

Our samples are fabricated from a molecular beam epitaxially-grown GaAs/AlGaAs heterostructure. It contains a two-dimensional electron gas (2DEG) located 200 nm below the surface. The 2DEG mobility at 4K is  $5.5 \cdot 10^6 \text{ cm}^2/\text{Vs}$  and the carrier density is  $1.43 \cdot 10^{11} \text{ cm}^{-2}$ .

A novel sample design realizes the theoretically pro-

posed scheme with independent injector and detector [6], see Fig. 1, (a). Each sample has two macroscopic ( $\sim 0.5 \times 0.5 \text{ mm}^2$ ) etched regions inside, separated by  $300 \mu\text{m}$  distance. Ohmic contacts are placed at the mesa edges. A split-gate partially encircles the etched areas, leaving uncovered two  $L = 5 \mu\text{m}$  wide gate-gap regions at the outer mesa edge, situated at  $30 \mu\text{m}$  distance.

Edge states (ES) were originally introduced as one-dimensional intersections of the Fermi level and filled Landau levels [7]. In samples with smooth edge profile, ES are represented by the compressible strips of finite width [8]. At the bulk filling factor  $\nu = 2$ , two co-propagating ES are separated in a gate-gap region by the incompressible strip with constant local filling factor  $\nu_c = 1$ . We deplete 2DEG under the gate to the same filling factor  $g = 1$ , so  $\nu_c = 1$  incompressible state fully separates the outer and two inner edges. They are only connected by the inter-ES transport in the gate-gap junctions. The maximum junction resistance does not exceed  $R \sim (h/e^2)l_{eq}/L \sim 3 \text{ MOhm}$ , where  $l_{eq}/L \sim 100$  is the ratio of the maximum equilibration length [10]  $l_{eq}$  to the gate-gap width  $L$ . Because of finite  $R$ , one can expect  $\mu_{out} = \mu_{in}$  for the electrochemical potentials of the outer and inner edges in the equilibrium.

In the present experiment, we enforce inter-ES transport in one gate-gap junction (injector), by applying *dc current* between the outer contact labeled as 3 and one of the inner contacts (the ground) see Fig. 1. It causes the energy dissipation in the injector. An independent gate-gap junction serves as a detector: the energy (in a form of plasmon, non-equilibrium electron or phonon) can be absorbed here by stimulating inter-ES transitions, which would disturb the equilibrium  $\mu_{in} = \mu_{out}$  in the detector junction. Every ES is characterized by definite electrochemical potential [7, 8], which is constant along ES except for the regions of current injection (i.e. current contacts and the injector junction in Fig. 1). We trace ES potentials by high-impedance electrometers connected to ohmic contacts in Fig. 1.

In our setup with co-propagating ES, the normal mag-

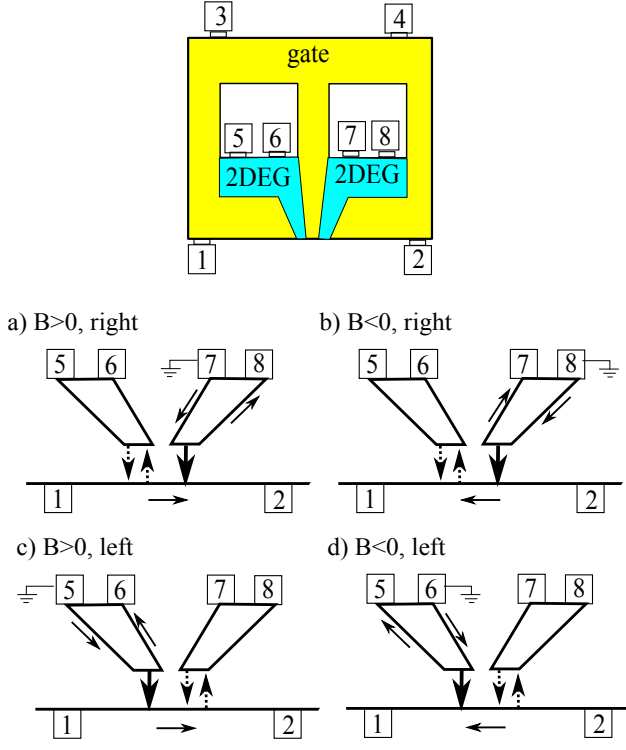


FIG. 1. (Color online) Schematic diagram of the sample (not in the scale, see the text). ES appear at the edges of etched regions (white), also at the border between the gate (yellow) and the uncovered 2DEG (light green). Ohmic contacts are denoted by bars with numbers. (a-d) Experimental configurations for two injector positions and two field directions. Thin arrows indicate electrons' drift along ES. Thick arrow denotes current in the injector junction. Dotted ones are for the equilibrium (forward and backward) transitions in the detector gate-gap.

netic field  $B$  defines the propagation direction for the charged transport along the outer mesa edge. There are four possible experimental configurations, depicted in Fig. 1 (a)-(d), which are labeled by the magnetic field sign ( $B > 0$  or  $B < 0$ ) and by the position (right or left) of the injector gate-gap junction.

The results presented below are independent of the cooling cycle. They are obtained in a dilution refrigerator at the base temperature of 30 mK. Standard two-point magnetoresistance is used to determine the electron concentration in the ungated area and to verify the contact quality. Magnetocapacitance measurements are used to find the available filling factors  $g$  under the gate.

The potentials of different Ohmic contacts are shown in Fig. 2 for integer filling factors  $\nu = 2, g = 1$  for all experimental configurations depicted in Fig. 1. The curves are obtained in a stationary regime (about 3 hours per curve).

In the detector gate-gap junction, we do observe the equilibrium ES electrochemical potential distribution  $\mu_{out} = \mu_{in}$  for two experimental configurations, see Fig 2

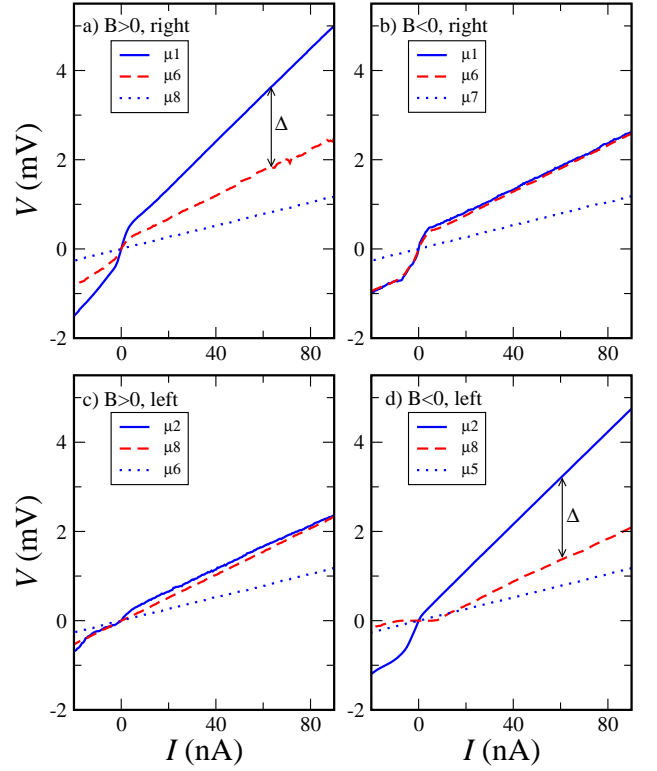


FIG. 2. (Color online) Potentials  $V_i$  of different Ohmic contacts ( $eV_i = \mu_i$ ) vs. injector current for the experimental configurations depicted in Fig. 1. Blue solid: potential  $\mu_{out}$  of the outer ES in the detector, which is also expected for the inner one in the equilibrium  $\mu_{out} = \mu_{in}$ . Red dash: measured potential of the inner ES  $\mu_{in}$  in the detector.  $\Delta$  denotes the difference  $e\Delta = \mu_{out} - \mu_{in}$ . Blue dots: the potential of the inner contact within the injector. Positive  $B = +3.72$  T and negative  $B = -3.51$  T fields differ in value because of different coolings. Filling factors are  $\nu = 2, g = 1$ .

(b) and (c). Our most astonishing experimental finding is the fact that in two other cases there is a non-zero difference  $e\Delta = (\mu_{out} - \mu_{in})$ , see Fig 2 (a) and (d). It occurs only if the detector is situated before the injector in a sense of the electrons' drift at the edge, *cp.* Fig. 1 (a) and (d). The effect is present for both signs of the applied current.

In our set-up, we not only know the direction of the electrons' drift in Fig 1, but can also obtain it directly from the experimental curves [9]. If the potential contact within the injector is situated so that electrons reach it before the ground, its potential reflects the current through the injector [9]. Since we apply a *current* through the junction, we do find this potential to be linear and independent on the experimental configuration in a full current range, see Fig. 2 (blue dots). In contrast, the potentials of the outer contacts demonstrate a clear non-linear behavior, see Fig. 2, because they are sensitive to the non-linear resistance of the injector gate-gap junction (see discussion below). The charge conservation for

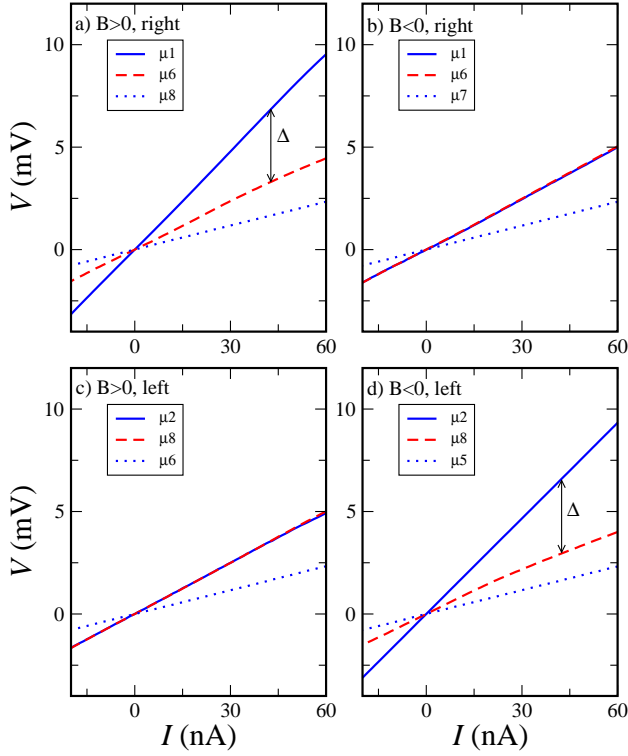


FIG. 3. (Color online) Potentials  $V_i$  of different Ohmic contacts ( $eV_i = \mu_i$ ) vs. injector current for the experimental configurations depicted in Fig. 1. Blue solid: potential  $\mu_{out}$  of the outer ES in the detector, which is also expected for the inner one in the equilibrium  $\mu_{out} = \mu_{in}$ . Red dash: measured potential of the inner ES  $\mu_{in}$  in the detector.  $\Delta$  denotes the difference  $e\Delta = \mu_{out} - \mu_{in}$ . Blue dots: the potential of the inner contact within the injector. Positive  $B = +11.15$  T and negative  $B = -10.53$  T fields differ in value because of different coolings. Filling factors are  $\nu = 2/3$ ,  $g = 1/3$ .

the injector junction demands an evident relation [9] between  $\mu_1$ ,  $\mu_2$  and the potential of the inner contact within the injector, which is indeed fulfilled for any experimental configuration. In this case, the fact that  $\mu_1^{right}$  for ( $B > 0$ ) exceeds  $\mu_1^{right}$  for ( $B < 0$ ) in Figs. 2,3 (a,b) indicates that electrons are propagating from the contact 1 to the contact 2 at the outer sample edge for the field which we denote as positive  $B > 0$ .

Similar results with non-linear curves are obtained for other bulk fillings with  $\nu_c = 1$ : ( $\nu = 3, g = 1$ ) and ( $\nu = 4/3, g = 1$ ). In contrast, the curves are linear for transport across  $\nu_c = 1/3$ , see Fig. 3, because of the smaller equilibration length [9]. However, Fig. 3 demonstrates finite  $\Delta$  for the same two experimental configurations for  $\nu_c = 1/3$ .

We can be sure that the detector is only connected with the injector through the edge. Zero  $\Delta$  in Figs. 2,3 (b,c) excludes a direct connection through the bulk, which would produce positive  $\Delta$  of the same order for all four experimental configurations. Similar effect would

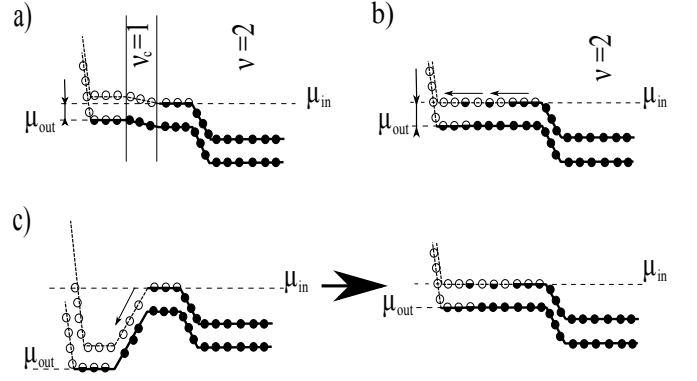


FIG. 4. (Color online) Schematic diagrams of the energy levels in the gate-gap junction at integer filling factors  $\nu = 2$ ,  $g = 1$ . Pinning of the Landau sublevels (solid) to the Fermi level (shot-dash) is shown in the compressible regions at electrochemical potentials  $\mu_{out}$  and  $\mu_{in}$ . Filled (half-filled) circles represent the fully (partially) occupied electron states. Open circles are for the empty ones. Arrows indicate electrons' transitions along the energy level. (a) Low imbalances  $eV = \mu_{out} - \mu_{in}$  across the incompressible strip. (b)  $eV$  reaches the spectral gap within  $\nu_c = 1$ . (c) Evolution of higher imbalance along the gate-gap edge.

be produced by a parasite ground within the detector region [11]. Fig. 3 also confirms the observed effect for an order of magnitude smaller detector resistance  $R = 6(h/e^2)$ .

Since there is no parasite connection between the injector and the detector, a finite  $\Delta$  in a stationary regime implies that the equilibrium is *dynamic* within the detector junction. The 'forward' inter-ES transitions, which tend to equilibrate ES (see below), should be compensated by some 'backward' ones. A necessary for  $\nu_c = 1$  change of electron's spin is easily provided by the spin-orbit coupling [10] and by the flip-flop process [9], but the energy for backward transitions can only be transferred from the injector. Thus, Figs. 2,3 demonstrate the energy transfer at the edge, contrary to the electrons' drift.

The energy transfer contrary to the electrons' drift can only be performed by neutral excitations such as non-equilibrium phonons and neutral collective modes. To make a choice, we start from the transport regimes across the injector gate-gap junction [9] for integer  $\nu_c$ :

(i) Low imbalances: ES electrochemical potential imbalance is much smaller than the energy gap in the  $\nu_c = 1$  incompressible strip, see Fig 4 (a). This regime corresponds to the initial (high-resistive with  $R \sim (h/e^2)l_{eq}/L$ ) parts of  $\mu_1, \mu_2$  in Fig. 2. Clearly different resistances of the right and the left gate-gap junctions are because of their different real widths  $L$ . This is an additional confirmation of the independence of two gate-gaps.

(ii) High imbalances: while the electrochemical potential difference reaches the spectral gap, see Fig. 4 (b),

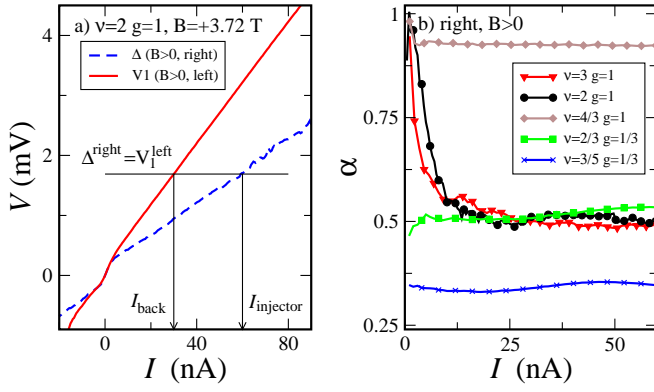


FIG. 5. (Color online) (a) Potential  $V_1 = \mu_1^{\text{left}}/e$  in comparison with  $\Delta^{\text{right}}$  for  $B > 0$ ,  $\nu = 2, g = 1$ . (b) Calculated  $\alpha = I_{\text{back}}/I_{\text{injector}}$  (see the text) as a function of  $I_{\text{injector}}$  for different filling factors,  $B > 0$ .

some electrons can be transferred between ES along the energy level and relax outside the gate-gap region. The junction resistance is diminished because of these elastic transitions. If higher imbalance is applied in the corner of the injector gate-gap in Fig. 1, it drops fastly (within 2-3  $\mu\text{m}$ ) [9], see Fig. 4 (c). This regime corresponds to the linear behavior of  $\mu_1$  and  $\mu_2$  in Fig. 2 at high currents.

We define a ratio  $\alpha = I_{\text{back}}/I_{\text{injector}}$ , which is a part of the 'backward' transitions in the detector in respect to the 'forward' ones in the injector.  $I_{\text{back}}$  is connected with the measured  $\Delta$  through the non-linear resistance of the detector gate-gap junction. The latter is fully determined by the ES structure and the gate-gap width, so it can be obtained from the ES imbalance in the injector in a symmetric configuration. We therefore determine  $\alpha$  as depicted in Fig. 5 (a). It's worth to mention, that both curves in Fig. 5 (a) change their slopes simultaneously, in contrast to, e.g., Fig. 2 (a). This is an additional argument that  $\Delta$  originates from the non-linear resistance of the detector junction.

Unity value of  $\alpha$  at low imbalances indicates a low dissipation of energy while transferred from the injector to the detector. If the transfer mechanism is the same, at high imbalances  $\alpha$  should reflect a part of non-elastic inter-ES transitions in the injector, which is confirmed by data in Fig. 5 (b). The data coincide for the filling factors  $\nu = 3, g = 1$  and  $\nu = 2, g = 1$  since the involved ES are separated by the same  $\nu_c = 1$  strip. Much higher  $\alpha$  for  $\nu = 4/3, g = 1$  reflects the fact that efficient elastic transitions are not reachable for the bulk  $\nu = 4/3$  [12]. For  $\nu_c = 1/3$  (at  $\nu = 2/3$  and  $3/5$ )  $\alpha$  is practically independent on the injector current. In this regime the linearity of the curves in Fig. 3 confirms [9] the presence of the gap at  $\nu_c = 1/3$ , and therefore non-elastic transitions in the injector.

It can be hardly imagined, that all the phonons emitted in the injector at low imbalances would be absorbed

in the detector, resulting in  $\alpha = 1$ . In contrast, plasmons are propagating along the edge and are characterized by low dissipation. The plasmon can not be responsible for the energy relaxation within ES [6, 13] in the quantum Hall regime, which is in a good agreement with the fact that the observed  $\Delta$  is only sensitive to the non-elastic transitions *within* the injector. In our setup it is a dipole (neutral) collective excitation which is created by an electron transition across the incompressible strip in Fig. 4. It do can propagate in the opposite direction along the interaction-reconstructed low-density edge of the  $\nu_c = 1, 1/3$  incompressible strip and its' dispersion allows to transfer a proper energy [4]. It is clear from the above consideration, that the excitation of this mode is only efficient at high imbalances in the process depicted in Fig. 4 (c), which is the main our difference from Ref. [1].

We wish to thank V.T. Dolgoplov, D.E. Feldman, D.G. Polyakov, D. A. Bagrets, and B. I. Halperin for fruitful discussions. We gratefully acknowledge financial support by the RFBR, RAS, the Program "The State Support of Leading Scientific Schools".

\* Corresponding author. E-mail: dev@issp.ac.ru

- [1] G. Granger, J. P. Eisenstein, J. L. Reno, Phys. Rev. Lett. 102, 086803 (2009).
- [2] Aveek Bid, Nissim Ofek, Hiroyuki Inoue, Moty Heiblum, Charles Kane, Vladimir Umansky, Diana Mahalu, Nature 466, 585, (2010).
- [3] C. L. Kane, M. P. A. Fisher, and Polchinski, Phys. Rev. Lett. 72, 4129 (1994); D. E. Feldman, F. Li, Phys. Rev. B 78, 161304-161307 (2008); E. Grosfeld, S. Das, Phys. Rev. Lett. 102, 106403 (2009); B. Rosenow and B. I. Halperin, Phys. Rev. B 81, 165313 (2010).
- [4] Xin Wan, E. H. Rezayi, and Kun Yang, Phys. Rev. B 68, 125307 (2003); C. d. C. Chamon and X. G. Wen, Phys. Rev. B 49, 8227 (1994).
- [5] J.P. Eisenstein, L.N. Pfeiffer, and K.W. West, Phys. Rev. Lett. 68, 674 (1992).
- [6] S. Takei, M. Millett, and B. Rosenow, Phys. Rev. B 82, 041306(R) (2010).
- [7] M. Büttiker, Phys. Rev. B 38, 9375 (1988).
- [8] D. B. Chklovskii, B. I. Shklovskii, and L. I. Glazman, Phys. Rev. B 46, 4026 (1992).
- [9] E. V. Deviatov, V. T. Dolgoplov, A. Wurtz, JETP Lett. 79, 618 (2004). For a review on inter-ES transport see E. V. Deviatov, A. Lorke, phys. stat. sol. (b) 245, 366 (2008).
- [10] G. Müller, D. Weiss, A. V. Khaetskii, K. von Klitzing, S. Koch, H. Nickel, W. Schlapp, and R. Lösch, Phys. Rev. B 45, 3932 (1992).
- [11] Even an unbelievable mistake in relative positions of the gate-gap regions would result in antisymmetric  $\Delta$  in respect to the magnetic field sign, which is inconsistent with zero  $\Delta$  in Figs. 2,3 (b,c).
- [12] E. V. Deviatov, A. Lorke, and W. Wegscheider, Phys. Rev. B 78, 035310 (2008).
- [13] D. A. Bagrets, I. V. Gornyi, and D. G. Polyakov, Phys.

Rev. B **80**, 113403 (2009)